Dalton Transactions

Cite this: *Dalton Trans.*, 2011, **40**, 4982

www.rsc.org/dalton

PAPER

Bis-imine-cyclometalated macrocycles: synthesis, characterization and observation of solution behaviour†

Hao Li, Ying-Feng Han and Guo-Xin Jin*

Received 12th October 2010, Accepted 24th February 2011
DOI: 10.1039/c0dt01377c

A novel class of cyclometalated macrocycles $[(Cp^*Ir)_2(R–N{=}C–C_6H_2–C{=}N–R)_2]_2$-$(pyrazine)_2\cdot(OTf)_4$ [R = Ph (**4a**), *p*-$MeOC_6H_4$ (**4b**), *p*-MeC_6H_4 (**4c**), *p*-ClC_6H_4 (**4d**), Me (**4e**)]; $[(Cp^*Rh)_2(R–N{=}C–C_6H_2–C{=}N–R)_2]_2(pyrazine)_2\cdot(OTf)_4$ [R = Ph (**4a′**), *p*-$MeOC_6H_4$ (**4b′**), *p*-MeC_6H_4 (**4c′**)] and $[(Cp^*Ir)_2(R–C{=}N–C_6H_4–N{=}C–R)_2]_2(pyrazine)_2\cdot(OTf)_4$ [R = Ph (**5a**), *p*-$MeOC_6H_4$ (**5b**)] was stepwise constructed through the double-site C–H activation of aromatic bis-imine substrates. The structures of binuclear complexes and tetranuclear macrocycles were confirmed by single-crystal X-ray diffraction. Isomers were found both in binuclear species and macrocyclic complexes. Flexible substrates led to the existence of isomers for binuclear species, yet gave no isomers after macrocyclic constructions; rigid ones, in contrast, led to isomers only for macrocyclic species. The isomers of tetranuclear macrocycles were thermodynamically stable to reversible transformation on a scale of days. Robust bonding and a certain degree of rigidity were invoked to explain the existence of isomers. This is the first example, to our knowledge, in which coordinated macrocycles containing half-sandwich Cp*M (M = Ir, Rh) fragments have been constructed, without a dynamic reversible process.

Introduction

Coordination-driven self-assembly has proven to be an efficient methodology for constructing well-defined metallosupramolecular macrocycles and cages.[1,2] In the past few years, several groups including those of Severin,[3] Therrien[4] and ourselves[5] have explored the use of Cp*M (M = Ir, Rh) and (*p*-cymene)Ru units as building blocks for discrete architectures. These half-sandwich units have advantages in solubility, thermal stability and flexibility in fine-tuning processes, and therefore, are suitable candidates for metallosupramolecular assembly.[3] As recent research has revealed, macrocycles/cages which contain Cp*M (M = Ir, Rh) or (*p*-cymene)Ru groups show potential in selective guest encapsulation,[6] cation/anion recognition[7] and drug delivery.[8]

The synthetic route to macrocycles containing half-sandwich metals developed by our group involves "chelating and bridging ligand" (Fig. 1), with two pairs of chelating site linking two metal atoms.[5,9] The macrocycle-constructing capabilities of such ligands, with different coordinating sites, including O^O–O^O[5,9a,b] and O^N–O^N,[9c,d] were investigated. Recently, we have reported that the C–H activation of aromatic imines can direct the iridium-mediated self-assembly, forming tetranuclear macrocycles (Scheme 1).[10] The most important feature about such macrocycles, compared with those containing the "chelating and bridging ligands", is the replacement of relatively dynamic M–O or M–N bonds by robust M–C bonds. This can lead to an increase of the structural stability.

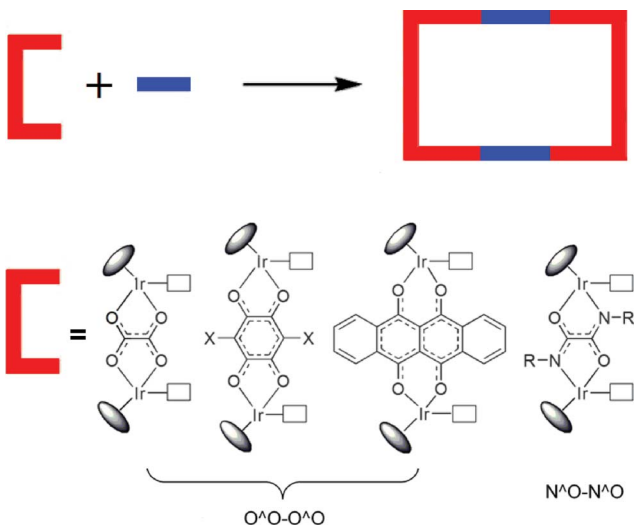

Fig. 1 Synthetic route of half-sandwich macrocycles using "chelating and bridging ligands" as building blocks.

To investigate the influence of M–C bonds on the metallosupramolecular macrocyclic systems, we designed a series of

Shanghai Key Laboratory of Molecular Catalysis and Innovative Material, Department of Chemistry, Fudan University, 200433, Shanghai, P. R. China. E-mail: gxjin@fudan.edu.cn; Fax: +86-21-65641740; Tel: +86-21-65643776

† CCDC reference numbers 744133 (**1a**), No. 744134 (**1b**), No. 744135 (**1b′**), 744140 (**2a**), 744141 (**2b**), 744136 (**3a**), 744137 (**3b**), 744138 (**3c**), 744139 (**3c′**) and 744142 (**4a**). For ESI and crystallographic data in CIF or other electronic format see DOI: 10.1039/c0dt01377c. For crystallographic data in CIF or other electronic format see DOI: 10.1039/c0dt01377c

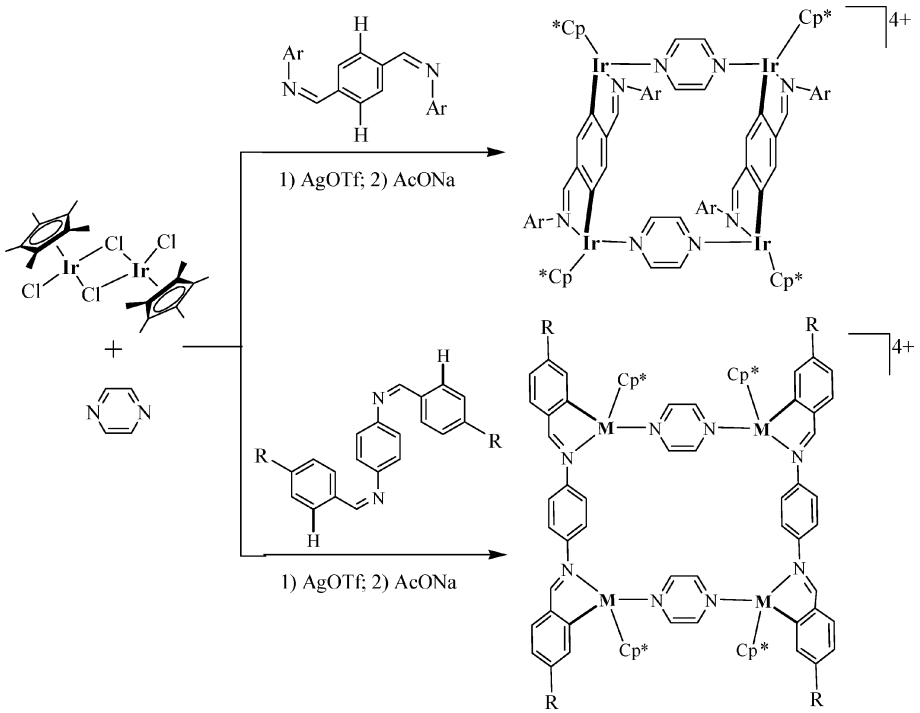

Scheme 1 Synthesis of bis-imine-cyclometalated macrocycles.

bis-imine substrates (Fig. 2), which may provide different degrees of rigidities to the cyclic structures. Detailed observations were also performed on the solution behaviours of the resulting cyclic complexes. Herein, we report the full characterization and further exploration of the bis-imine-containing organometallic macrocycles. Isomers of tetranuclear macrocycles were observed when ligands provide both high rigidity and structural stability, and are not be found when ligands contain rotation axes or labile coordinate bonds to the metal centers.

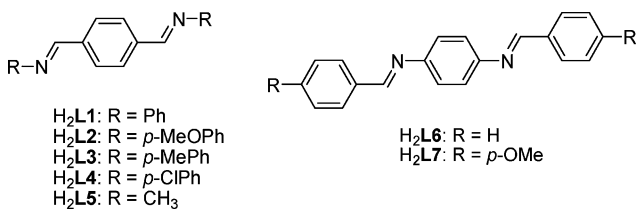

Fig. 2 Structures of bis-imine substrates.

Results and discussion

Bis-imine substrates H_2**L1**–H_2**L7** can be synthesized using the Schiff-base condensation reaction.[11] When undergoing the cyclometalation, **L1–L5** will give completely rigid structures, whereas **L6** and **L7** will give free rotation axes, allowing the change of directions between two metal centres.

Binuclear cyclometalated complexes of 1a–1e and 1a′–1c′

Davies *et al.* have reported the C–H activation of aromatic imine substrates in the presence of sodium acetate.[12] The acetate ion is believed to act as both catalyst and base, promoting the facile cleavage of the C–H bond at room temperature.[13] In light of the Davies' work, we performed analogous reactions based on bis-imine substrate **L1–L5**.

When **L1** was treated with $[Cp^*IrCl_2]_2$ in the presence of an excess of sodium acetate, significant change of colour was observed from orange to dark red, affording the dark red solid **1a** in moderate yields (Scheme 2). The ^{1}H NMR spectrum indicates that two C–H bonds in the middle phenyl group were activated, which was also confirmed by the single crystal structure. The two activated C–H bonds were *para*, probably due to a steric hindrance effect (Fig. 3a). The two Cp* groups and two Cl atoms adopted *trans*-conformation, respectively, which minimized the energy of the structure. The Ir–$N_{CH=N}$, Ir–C_{Ar} bond lengths and the C_{Ar}–Ir–$N_{CH=N}$ angles are typical compared with those of reported Cp*Ir cyclometalated complexes.[12,14]

Ligands **L2–L5** could also undergo the same kind of reactions, affording **1b–1e** as major products. Effects of substituent groups on the speed of reactions were observed (Scheme 2). For **L2** and **L3**, which contain strong electron-donor groups, the double-site cyclometalations occurred more quickly, whereas the rate of formation of electron-acceptor-containing **1d** was relatively slow. This result could be explained by the different electron densities at the N atoms, which affect the coordinating abilities.[15] The Cp*Rh group also proved to be capable of mediating the double-site cyclometalations, giving **1a′–1c′** as major products (Scheme 2). However, the reaction rates were lower than those of Cp*Ir. Single crystal structures of **1b** and **1b′** were obtained (Fig. 3b, c).

Interestingly, two cyclometalation reactions of the same phenyl group seemed favoured. When $[Cp^*IrCl_2]_2$ and **L1** reacted in the ratio of 1 : 2, the major product was still **1b**. Although favored stoichiometrically, no mono-cyclometalated product was found.

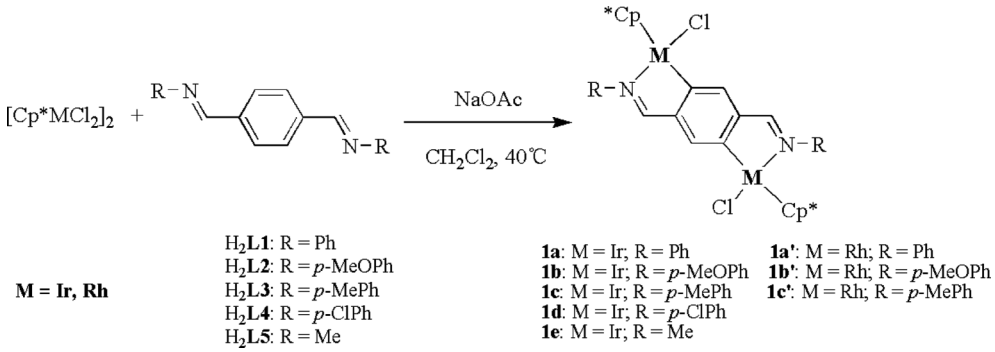

Scheme 2 Synthesis of **1a–1e** and **1a′–1c′**.

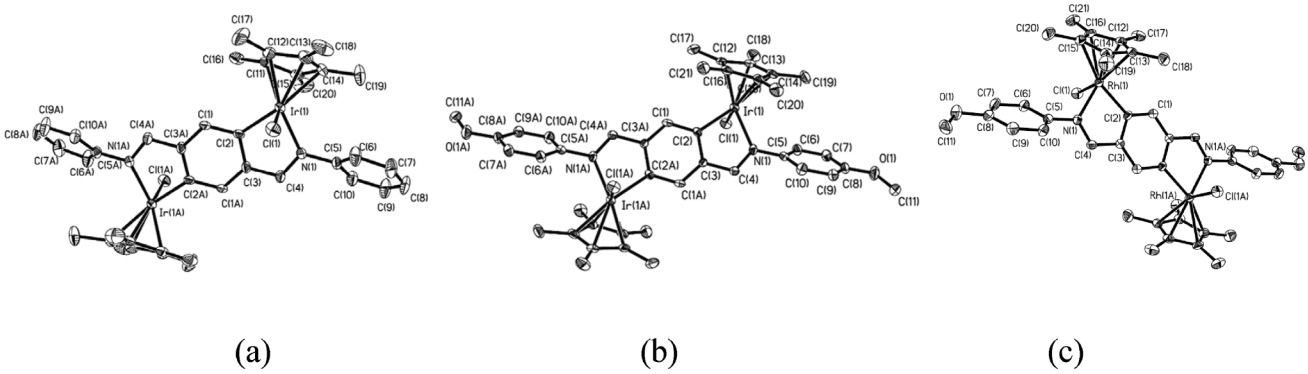

Fig. 3 (a) ORTEP view of **1a** (ellipsoids at the 30% probability level). Hydrogen atoms have been omitted for clarity. Selected bond lengths (Å) and angles (°): Ir(1)–C(2) 2.029(4), Ir(1)–N(1) 2.102(4); C(2)–Ir(1)–N(1) 77.54(15), C(4)–N(1)–Ir(1) 115.8(3). (b) ORTEP view of **1b**. Selected bond lengths (Å) and angles (°): Ir(1)–C(2) 2.049(1), Ir(1)–N(1) 2.096(8); C(2)–Ir(1)–N(1) 77.60(41), C(4)–N(1)–Ir(1) 116.6(8). (c) ORTEP view of **1b′**. Selected bond lengths (Å) and angles (°): Rh(1)–C(2) 2.028(6), Rh(1)–N(1) 2.095(6); C(2)–Rh(1)–N(1) 78.41(21), C(4)–N(1)–Rh(1) 115.2(7).

Binuclear cyclometalated complexes of 2a and 2b

Similarly to those of **L1–L5**, cyclometalations of **L6** and **L7** were performed in the presence of NaOAc, affording **2a** and **2b**, respectively (Scheme 3). The structures of **2a** and **2b** were confirmed by single-crystal X-ray diffraction, showing that the C–H activations occurred at the *ortho*-sites of two imine groups (Fig. 4).

However, unlike the completely rigid species of complexes **1a–e**, both **2a** and **2b** gave evidence of isomers in solution. In the ^{1}H NMR spectra of **2a** (Fig. 5), peaks attributed to the CH═N group and the Cp* groups were split into two equal parts, indicating different chemical environments of the phenyl group. The existence of isomers is probably due to the different configurations of the metal atoms (Fig. 5). A similar phenomenon does not occur for **1a–e** and **1a′–1c′**.

Synthesis and characterization of tetranuclear bis-imine-cyclometalated macrocycles

Macrocycle-constructed reactions were performed, using the binuclear cyclometalated species as building blocks. After the treatment with AgOTf, **1a–1e** can reacted with bridging pyrazine ligands, affording **3a–3e**, respectively (Scheme 4). ^{1}H NMR indicated that the bis-imine substrates and bridging ligands were in a 1 : 1 ratio. Single-crystal X-ray diffraction studies for **3a–3c** showed tetranuclear macrocyclic structures (Fig. 6). **3a–3c** were almost square, with dimensions of 6.96 and 6.98 Å for Ir···Ir non-bonding distances in **3a** and very similar dimensions for **3b** and **3c**. In all the three structures, the two middle phenyl groups in the bis-imine substrates were parallel to each other, respectively, as well as two pyrazine ligands. Cp*Rh-containing macrocycles can also be synthesized using a similar protocol (Scheme 4), affording

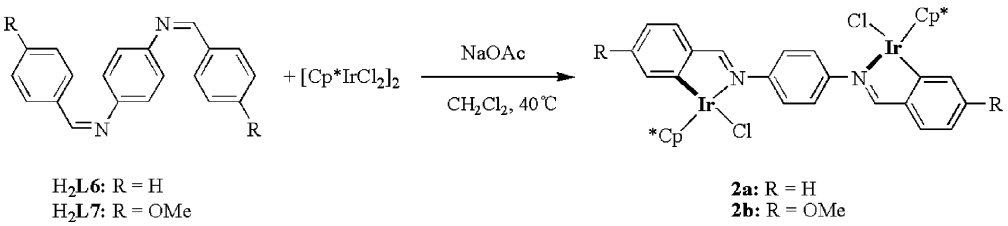

Scheme 3 Synthesis of **2a** and **2b**.

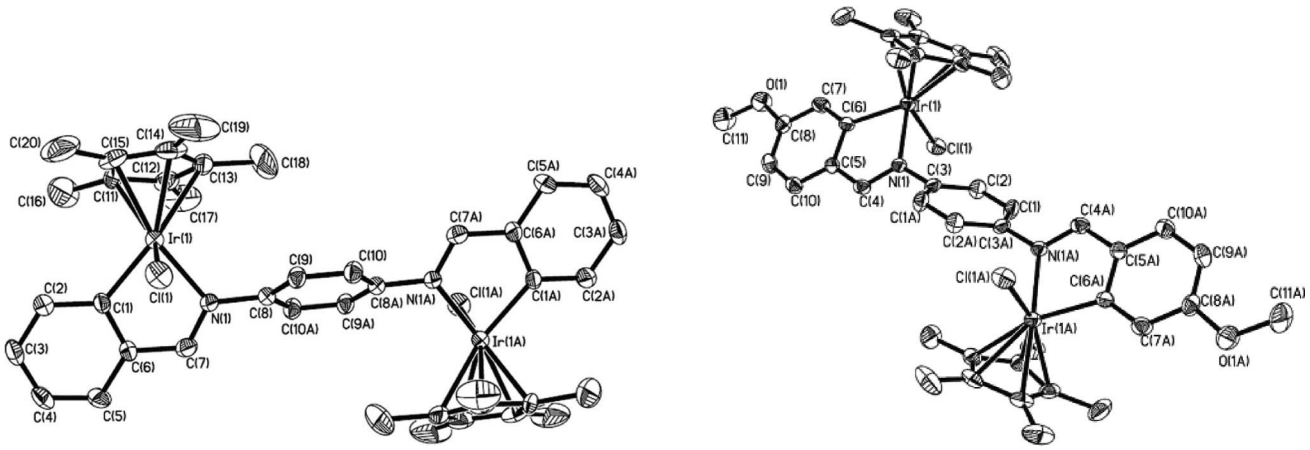

Fig. 4 (a) ORTEP view of **2a** (ellipsoids at the 30% probability level). Hydrogen atoms have been omitted for clarity. Selected bond lengths (Å) and angles (°): Ir(1)–C(1) 2.030(6), Ir(1)–N(1) 2.092(4), N(1)–C(7) 1.292(7); C(1)–Ir(1)–N(1) 78.1(2). (b) ORTEP view of **2b**. Selected bond lengths (Å) and angles (°): Ir(1)–C(1) 2.049(1), Ir(1)–N(1) 2.096(8), N(1)–C(7) 1.289(5); C(1)–Ir(1)–N(1) 77.6(0).

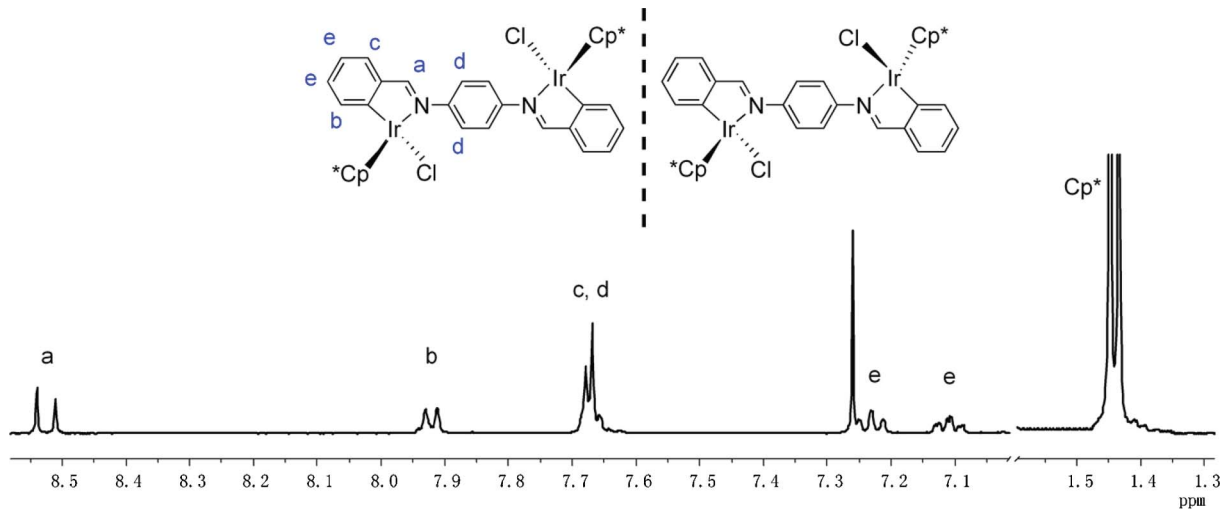

Fig. 5 Top: two proposed structures of isomers of **2a**; bottom: ^{1}H NMR spectrum of **2a** in $CDCl_3$.

3a′–3c′. The single-crystal structure of **3c′** reveals a tetranuclear cyclic structure, similar to those of **3a–3c** (Fig. 6d).

Complexes **2a** and **2b** could also react with pyrazine, after treatment with AgOTf, giving **4a** and **4b** as products, respectively (Scheme 5). Significant change of colour from yellow to red after the addition of pyrazine indicated the coordination of N atoms to the Ir centres. A tetranuclear rectangular single-crystal structure of **4a** was obtained (Fig. 7), with the dimensions of

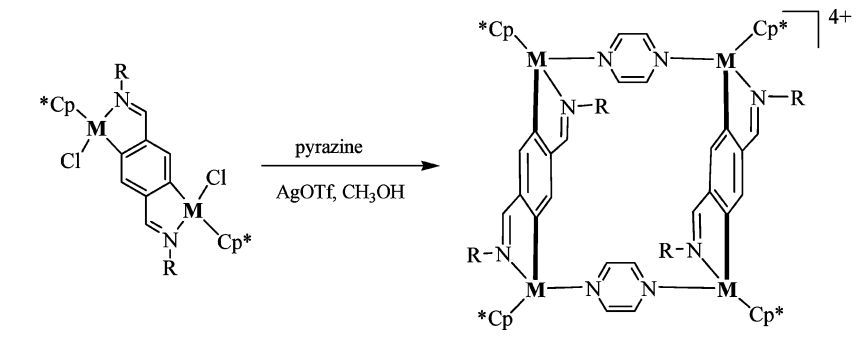

1a: M = Ir, R = Ph
1b: M = Ir, R = *p*-MeOPh
1c: M = Ir, R = *p*-MePh
1d: M = Ir, R = *p*-ClPh
1e: M = Ir, R = Me
1a′: M = Rh, R = Ph
1b′: M = Rh, R = *p*-MeOPh
1c′: M = Rh, R = *p*-MePh

3a: M = Ir, R = Ph
3b: M = Ir, R = *p*-MeOPh
3c: M = Ir, R = *p*-MePh
3d: M = Ir, R = *p*-ClPh
3e: M = Ir, R = Me
3a′: M = Rh, R = Ph
3b′: M = Rh, R = *p*-MeOPh
3c′: M = Rh, R = *p*-MePh

Scheme 4 Synthesis of **3a–3e** and **3a′–3c′**.

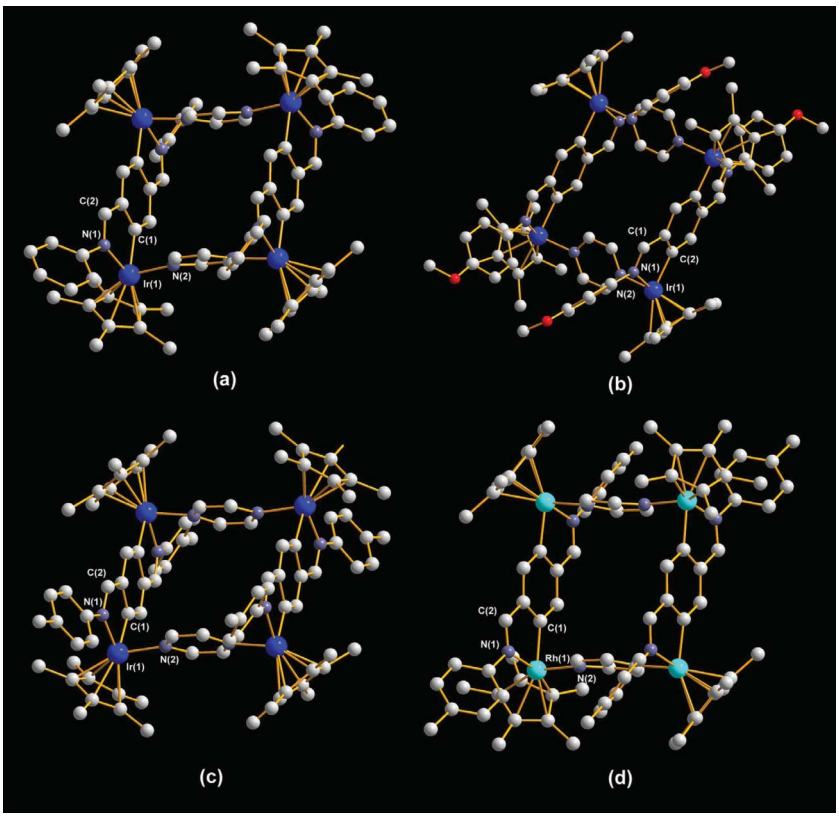

Fig. 6 (a) Complex cation of **3a** (C: gray, N: blue gray, O: red, Ir: blue). Selected bond lengths (Å) and angles (°): Ir(1)–C(1) 2.073(0), Ir(1)–N(1) 2.064(5), Ir(1)–N(2) 2.142(5), N(1)–C(2) 1.310(2); C(1)–Ir(1)–N(1) 77.2(6), N(1)–Ir(1)–N(2) 89.9(6), C(1)–Ir(1)–N(2) 86.0(2), (b) Complex cation of **3b**. Selected bond lengths (Å) and angles (°): Ir(1)–C(1) 2.019(9), Ir(1)–N(1) 2.067(1), Ir(1)–N(2) 2.083(2), N(1)–C(2) 1.292(6); C(1)–Ir(1)–N(1) 77.9(1), N(1)–Ir(1)–N(2) 87.0(5), C(1)–Ir(1)–N(2) 88.5(5). (c) Complex cation of **3c**. Selected bond lengths (Å) and angles (°): Ir(1)–C(1) 2.070(2), Ir(1)–N(1) 2.068(6), Ir(1)–N(2) 2.113(1), N(1)–C(2) 1.257(3); C(1)–Ir(1)–N(1) 78.8(6), N(1)–Ir(1)–N(2) 87.1(6), C(1)–Ir(1)–N(2) 86.0(8). (d) Complex cation of **3c′** (C: gray, N: blue gray, O: red, Rh: turquoise). Selected bond lengths (Å) and angles (°): Rh(1)–C(1) 2.022(9), Rh(1)–N(1) 2.078(3), Rh(1)–N(2) 2.095(6), N(1)–C(2) 1.272(5); C(1)–Rh(1)–N(1) 78.4(3), N(1)–Rh(1)–N(2) 90.2(9), C(1)–Rh(1)–N(2) 87.1(5).

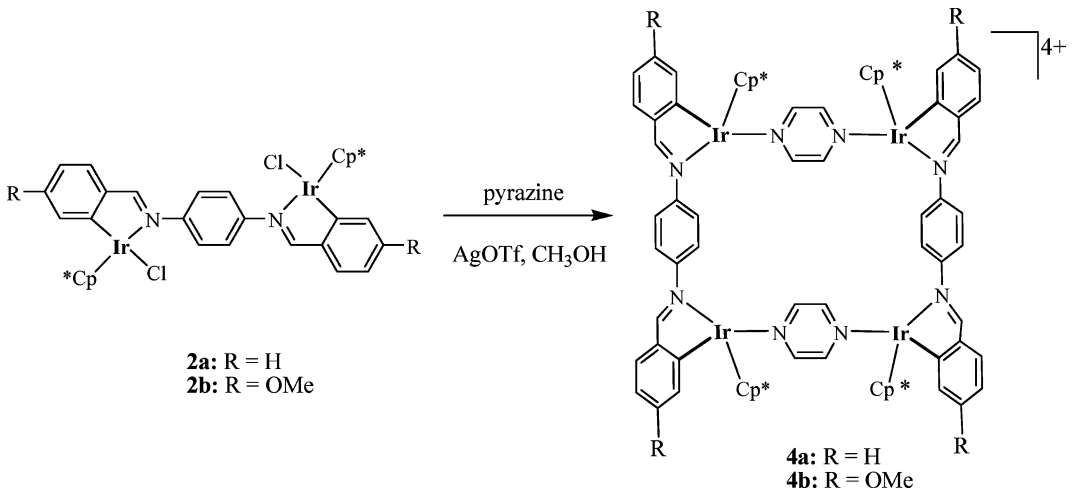

Scheme 5 Synthesis of **4a** and **4b**.

8.4 and 7.0 Å for the Ir···Ir non-bonding distances. Different from those in the binuclear species, the Cp* groups in the crystal structure of **4a** faced inward and partially filled one side of the macrocycle, so forming a half-open cavity in which two OTf ions were encapsulated. Guest ion **A** was surrounded by four Cp* groups, with a distance of 2.60 Å between the O atom in OTf ion and H atom in the nearest methyl group of Cp*, indicating a weak intermolecular hydrogen bond. The other guest ion **B** was in between two bis-imine fragments. The middle phenyl groups of the bis-imine fragments were facing the guest ion, with a distance

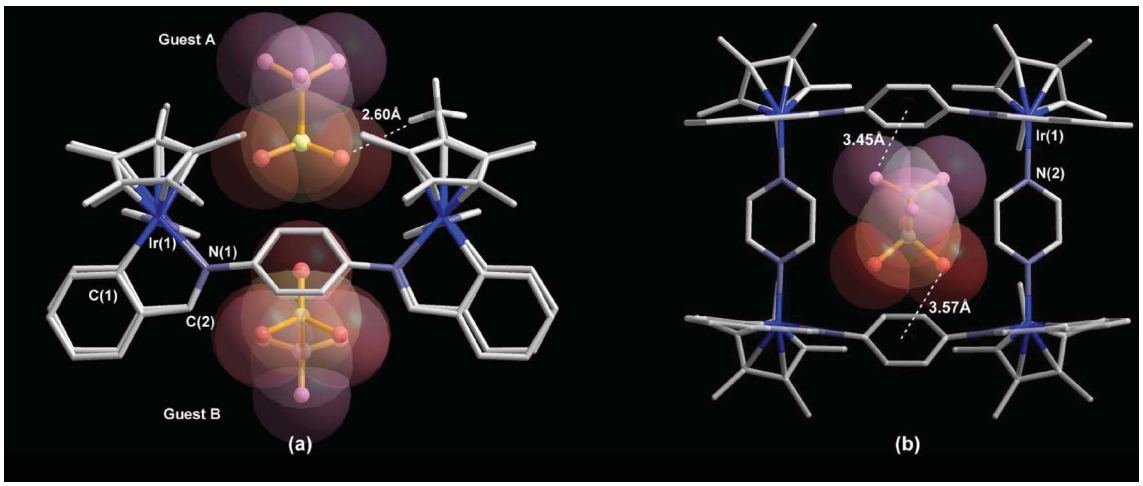

Fig. 7 (a) Side views of complex cation of **4a** (C: gray, N: blue gray, O: red, F: pink, S: yellow, Ir: blue). Selected bond lengths (Å) and angles (°): Ir(1)–C(1) 2.043(9), Ir(1)–N(1) 2.120(5), Ir(1)–N(2) 2.123(3), N(1)–C(2) 1.277(4); C(1)–Ir(1)–N(1) 77.9(4), N(1)–Ir(1)–N(2) 88.4(9), C(1)–Ir(1)–N(2) 84.1(5). (b) Top view of the complex cation of **4a**.

of 3.45 Å between the centre of one phenyl group and F atoms of guest ion, and 3.57 Å between the centre of the other phenyl group and O atoms of OTf ion.

Solution behaviour of bis-imine-containing tetranuclear macrocycles

One obvious feature about the bis-imine activated macrocycles was the robust bonding of metal centres and organic ligands/substrates. Hence these cyclometalation-containing macrocycles show higher structural stability compared with those containing Ir–O or Rh–O bonds reported previously by us and other groups.[3–8] Observations were performed to elucidate effects of stabilities on solution behaviours.

The ^{1}H NMR spectra of **3a–3e** and **3a′–3c′** (Fig. 8a shows the example of **3e**) showed equal splitting of all the peaks when using $CDCl_3$ as solvent. Further investigations were employed for **3e** (**3e** was chosen because it gives the simplest ^{1}H NMR spectrum), and demonstrated that the phenomenon could be explained by existence of isomer pairs in a ratio of 1 : 1. One of the isomers had a poor solubility in CH_3OH (which is also the reason why it was not detected and reported at the first place:[10] this isomer is barely detectable by ^{1}H NMR when using CD_3OD as solvent) but had a good solubility in $CHCl_3$; the other one, on the contrary, had a much poorer solubility in $CHCl_3$ and a better one in CH_3OH. Separations of the two isomers were realized by repeated recrystallization from $CHCl_3$. In the ^{1}H NMR spectra of the separated isomers, no division of any peaks occurred. It was worth noting that a high energy barrier between those pairs of isomers was indicated since no sign of in-solution transformation between isomers was detected, even after days of heating in 40 °C. Significant change of chemical shift in the ^{1}H NMR spectra of the separated isomers were found when using $CDCl_3$ and CD_3OD as solvent, respectively (Fig. 8b), due to the difference of polarities of solvents.

However, for the cases of **4a** and **4b**, no sign of isomers was observed in ^{1}H NMR (Fig. 9). Highly symmetrical structures were indicated, as no splitting for the four CH═N groups were found in their NMR spectra.

A proposed two-side attack is proposed for the existence of isomers for **3a–3e** and **3a′–3c′**. After the dissociation of M–Cl bonds in the binuclear complex, the metal centres could be attacked by the N atom of pyrazine from either side of the planar bis-imine substrate. Therefore, when metal centre A and B from two different binuclear fragments were connected by the bridging ligand, the configuration of them could be the same or different, as a consequence of the two-side attack (Fig. 10a). The configurations of A′ and B′—the other metal atoms of each binuclear complex—were determined by those of metal centre A and B, because of the rigid structure of **L1–L5**. Thus, two isomers were formed and could not transform easily, since the transformation of configurations requires the breaking of two relatively robust Ir–N/Rh–N bonds at the same time, which was unlikely to happen (Fig. 10b).

This explanation is supported by our group's previous results,[9,16] in which no tetranuclear macrocycles showed similar evidence of isomers. This might be owing to the reasons below: (i) the highly symmetrical structure of the binuclear building blocks will not give different configurations with pyrazine attack the metal centres from different sides,[9a,b] and (ii) the relatively weak M–O bonds might be easily broken, allowing the facile transformation of different configurations. It is noticeable that M–C bond cannot guarantee the existence of isomers, for one of our group's reported terephthalic-acid-cyclometalated macrocycles also showed no evidence of isomers[16] and may indicate that the existence of M–O bonds was one of the key factors for the absence of isomers.

Rigidity should also be considered to explain why no isomers were present for **4a** and **4b**. The binuclear building blocks of them exhibited free rotation axes, so that the determination of one metal centre's configuration had no effect on the other. Therefore, one favorable configuration of the macrocyclic structure could be obtained from the stepwise transformation of each metal centre, which only required the cleavage of one Ir–N/Rh–N bond. Steric hindrance or template effect of guest ions might also be a driving

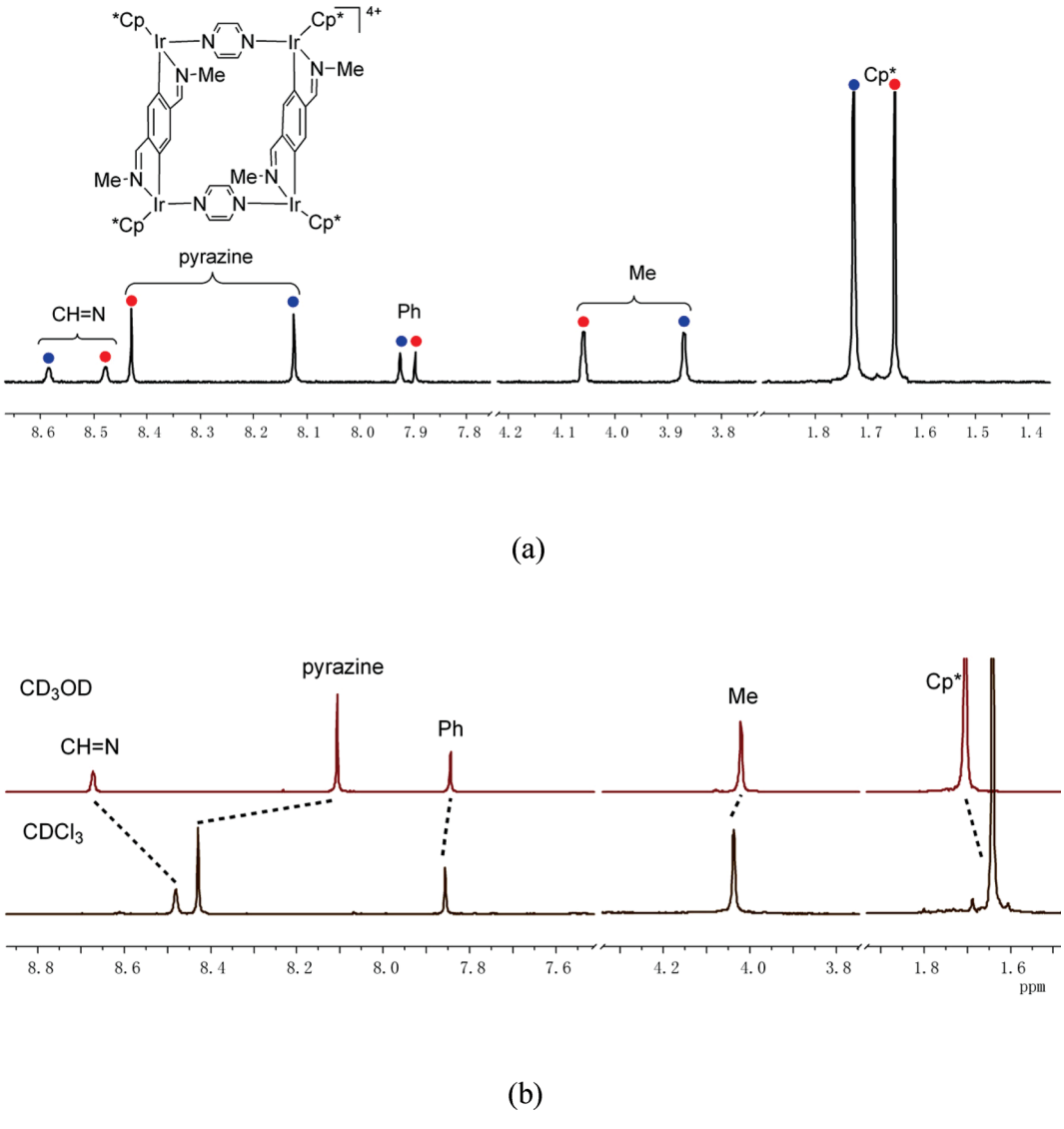

Fig. 8 (a) ^{1}H NMR spectrum of isomers of **3e** in $CDCl_3$, blue and red spots correspond to the two different isomers as determined by NMR of separated isomers. (b) ^{1}H NMR spectra of a separated isomer of **3e** in $CDCl_3$ and CD_3OD as solvent.

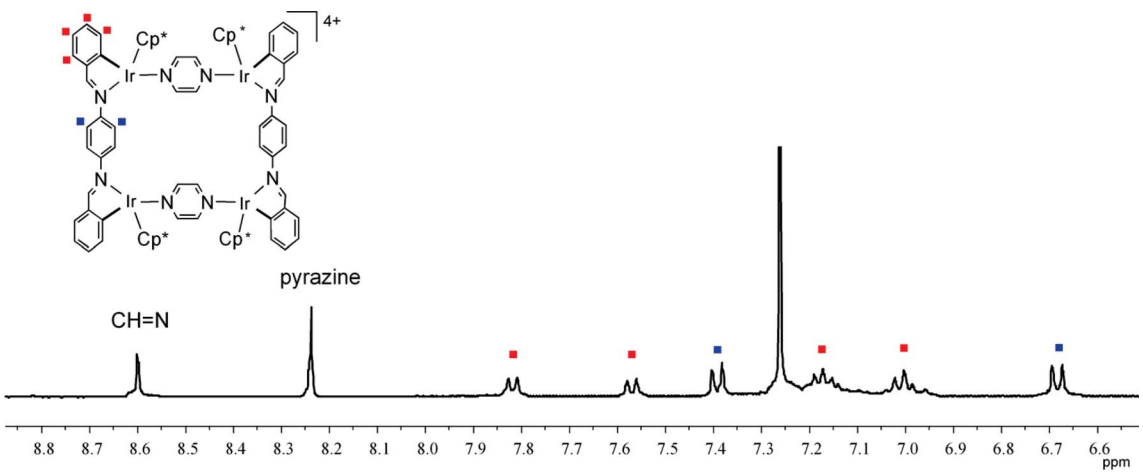

Fig. 9 (a) ^{1}H NMR spectrum of **6a** in $CDCl_3$ and (b) ^{1}H NMR spectrum of **7** in CD_3OD.

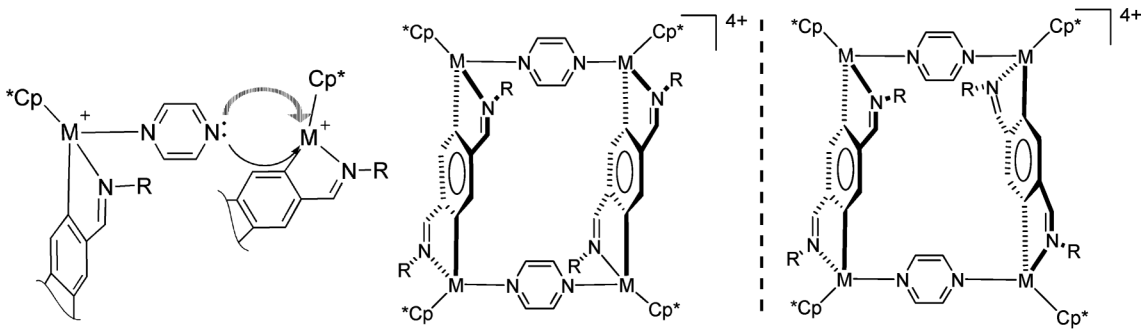

(a) (b)

Fig. 10 (a) Proposed two-side attack process and (b) proposed structures of tetranuclear isomers.

force, as indicated by the crystal structure of **4a**. An increase of flexibility should also aid a favorable configuration to be obtained.

Conclusion

Stepwise constructions of bis-imine-cyclometalated macrocycles were investigated. The synthetic route was established for various substrates (**L1–L7**) and metal fragments (Cp*Ir or Cp*Rh). The structures of binuclear complexes and tetranuclear macrocycles were confirmed by single-crystal X-ray diffraction. Isomers were found both in binuclear species and macrocyclic complexes. More flexible substrates led to the existence of isomers of binuclear species, yet gave no isomers after macrocyclic construction; rigid substrates, in contrast, led to isomers only for macrocyclic species. The isomers of tetranuclear macrocycles were thermodynamically stable to reversible transformation on a scale of days. Robust bonding and a degree of rigidity were proposed as requirements for the existence of isomers. This is the first example, to our knowledge, that coordinate macrocycles containing half-sandwich Cp*M (M = Ir, Rh) fragments were constructed, without showing a dynamic reversible process. The results may help in understanding the influence of M–C bonds on the solution behaviour of coordinate macrocycles, while and the stability of this type of bis-imine-cyclometaled macrocycle may benefit future researches, such as in controllable release of guest molecules.

Experimental

General procedures and materials

All reactions and manipulations were performed under a nitrogen atmosphere, using standard Schlenk techniques. However, once the reactions were completed, subsequent work-ups were done without precaution, as the compounds are air-stable. Solvents were purified by standard methods prior to use. $[Cp^*IrCl_2]_2$ was prepared according to the reported procedures.[17] ^{1}H NMR spectra were measured on a VAVCE-DMX 400 Spectrometer in CD_3OD or $CDCl_3$. Elemental analysis was performed on Elementar vario EL III Analyzer. IR (KBr) spectra were recorded on the Nicolet FT-IR spectrophotometer.

Synthesis of bis-imine ligand L1–L7

The bis-imine ligands **L1–L7** were prepared from a modified method of literature procedures.[11] Corresponding aldehydes and amines were reacted in a ratio of 1 : 2 in chloroform overnight at room temperature. Solid products were obtained after the removal of solvent, an after washing in CH_3OH several times. ^{1}H NMR spectra were consistent with reported ones for **L1**,[11a] **L2**,[11b] **L3**,[11b] **L5**[11a] and **L6**.[11c]

L1: Yellow, yield: 88%. ^{1}H NMR (400 MHz, $CDCl_3$, ppm) δ 8.42 (s, 2H, HC═N); 8.10 (s, 4H); 7.57 (d, 4H); 7.42 (m, 4H); 7.30 (m, 2H).

L2: Yellow, yield: 90%. ^{1}H NMR (400 MHz, $CDCl_3$, ppm) δ 8.54 (s, 2H, HC═N); 8.00 (s, 4H); 7.27 (d, 4H); 6.95 (d, 4H); 3.86 (s, 6H, OMe).

L3: Yellow, yield: 93%. ^{1}H NMR (400 MHz, $CDCl_3$, ppm) δ 8.53 (s, 2H, HC═N); 8.00 (s, 4H); 7.19 (m, 8H); 2.38 (s, 6H, Me).

L4: Yellow, yield: 91%. ^{1}H NMR (400 MHz, $CDCl_3$, ppm) δ 8.50 (s, 2H, HC═N); 8.01 (s, 4H); 7.36 (d, 4H); 7.20 (d, 4H).

L5: Pale yellow, yield: 90%. ^{1}H NMR (400 MHz, $CDCl_3$, ppm) δ 8.26 (s, 2H, HC═N); 7.71 (s, 4H, C_6H_4); 3.50 (s, 6H, Me).

L6: Yellow, yield: 82%. ^{1}H NMR (400 MHz, $CDCl_3$, ppm) δ 8.63 (s, 2H, HC═N); 7.94 (m, 4H); 7.50 (m, 6H); 7.33 (s, 4H).

L7: Yellow, yield: 92%. ^{1}H NMR (400 MHz, $CDCl_3$, ppm) δ 8.45 (s, 2H, HC═N); 7.86 (d, 4H); 7.25 (d, 4H); 6.99 (d, 4H); 3.86 (s, 6H, OMe).

Preparation of binuclear complexes 1a–1e and 1a′–1c′

A mixture of $[Cp^*MCl_2]_2$ (0.1 mmol, M = Ir, Rh), NaOAc (0.6 mmol), and corresponding substrates **L1–L5** (0.1 mmol) was stirred at 40 °C in 20 mL of dichloromethane for 8–18 h. The mixture was filtered and evaporated to afford black/dark red solids which were further purified by silica gel column chromatography (CH_2Cl_2–EA = 95 : 5) to afford pure cyclometalated compounds in yields of 70–78%.

1a: Black, 13 h, yield: 76%. Anal. Calc. for $C_{40}H_{44}Cl_2Ir_2N_2$: C 47.66, H 4.40, N 2.78. Found: C 47.58, H 4.37, N 2.83%. ^{1}H NMR (400 MHz, $CDCl_3$, ppm): δ 8.42 (s, 2H, HC═N); 8.10 (s, 2H); 7.58 (d, 4H); 7.42 (m, 4H); 7.31 (m, 2H); 1.45 (s, 30H, C_5Me_5). ^{13}C NMR ($CDCl_3$, ppm): δ 175.78 (Ir–C), 159.60 (HC═N), 152.03, 151.50, 135.38, 128.97, 127.35, 122.60, 88.97 (C_5Me_5), 8.85 (C_5Me_5). IR (KBr): $\nu_{C=N}$ = 1551 cm^{-1}.

1b: Dark red, 12 h, yield: 75%. Anal. Calc. for $C_{42}H_{48}Cl_2Ir_2N_2O_2$: C 47.23, H 4.53, N 2.62. Found: C 47.16, H 4.24, N 2.72%. ^{1}H NMR (400 MHz, $CDCl_3$, ppm): δ 8.36 (s, 2H, HC═N); 8.06 (s, 2H); 7.52 (d, 4H); 6.92 (d, 4H); 3.86 (s, 6H, OMe); 1.46 (s, 30H, C_5Me_5). ^{13}C NMR (400 MHz, $CDCl_3$–CD_3OD 4 : 1, 50 °C): δ 174.86 (Ir–C), 158.99 (HC═N), 158.74, 151.37, 145.28, 135.03, 123.46, 113.85, 88.88 (C_5Me_5), 55.39 (OMe), 8.58 (C_5Me_5). IR (KBr): $\nu_{C=N}$ = 1534 cm^{-1}.

1c: Dark red, 12 h, yield: 78%. Anal. Calc. for $C_{42}H_{48}Cl_2Ir_2N_2$: C 48.68, H 4.67, N 2.70. Found: C 48.45, H 4.39, N 2.83%. ^{1}H NMR (400 MHz, $CDCl_3$, ppm): δ 8.37 (s, 2H, HC═N); 8.07 (s, 2H); 7.45 (d, 4H); 7.20 (d, 4H); 2.41 (s, 6H, Me); 1.48 (s, 30H, C_5Me_5). IR (KBr): $\nu_{C=N}$ = 1560 cm^{-1}.

1d: Black, 18 h, yield: 70%. Anal. Calc. for $C_{40}H_{42}Cl_4Ir_2N_2$: C 44.61, H 3.93, N 2.60. Found: C 44.29, H 3.57, N 2.66%. ^{1}H NMR (400 MHz, $CDCl_3$, ppm): δ 8.39 (s, 2H, HC═N); 8.10 (s, 2H); 7.54 (d, 4H); 7.40 (d, 4H); 1.50 (s, 30H, C_5Me_5). IR (KBr): $\nu_{C=N}$ = 1556 cm^{-1}.

1e: Dark red, 8 h, yield: 78%. Anal. Calc. for $C_{30}H_{40}Cl_2Ir_2N_2$: C 40.76, H 4.56, N 3.17. Found: C 40.39, H 4.77, N 3.26%. ^{1}H NMR (400 MHz, $CDCl_3$, ppm): δ 8.31 (s, 2H, HC═N); 7.88 (s, 2H); 3.91 (t, 6H); 1.71 (s, 30H, C_5Me_5). IR (KBr): $\nu_{C=N}$ = 1560 cm^{-1}.

1a′: Dark red, 18 h, yield: 71%. Anal. Calc. for $C_{40}H_{44}Cl_2Rh_2N_2$: C 57.92, H 5.35, N 3.38. Found: C 57.58, H 5.37, N 3.23%. ^{1}H NMR (400 MHz, $CDCl_3$, ppm): δ 8.42 (s, 2H, HC═N); 8.10 (s, 2H); 7.58 (d, 4H); 7.42 (m, 4H); 7.31 (m, 2H); 1.45 (s, 30H, C_5Me_5). IR (KBr): $\nu_{C=N}$ = 1550 cm^{-1}.

1b′: Dark red, 12 h, yield: 68%. Anal. Calc. for $C_{42}H_{48}Cl_2Rh_2N_2O_2$: C 56.71, H 5.44, N 3.15. Found: C 56.66, H 5.24, N 3.12%. ^{1}H NMR (400 MHz, $CDCl_3$, ppm): δ 8.36 (s, 2H, HC═N); 8.04 (s, 2H); 7.50 (d, 4H); 6.90 (d, 4H); 3.79 (s, 6H, OMe); 1.50 (s, 30H, C_5Me_5). IR (KBr): $\nu_{C=N}$ = 1538 cm^{-1}.

1c′: Dark red, 12 h, yield: 72%. Anal. Calc. for $C_{42}H_{48}Cl_2Rh_2N_2$: C 58.82, H 5.64, N 3.27. Found: C 58.59, H 5.60, N 3.41. ^{1}H NMR (400 MHz, $CDCl_3$, ppm): δ 8.32 (s, 2H, HC═N); 8.01 (s, 2H); 7.42 (d, 4H); 7.21 (d, 4H); 2.40 (s, 6H, Me); 1.47 (s, 30H, C_5Me_5). IR (KBr): $\nu_{C=N}$ = 1561 cm^{-1}.

Preparation of binuclear complexes 2a and 2b

A mixture of $[Cp^*IrCl_2]_2$ (0.1 mmol), NaOAc (0.6 mmol), and corresponding substrates **L6** or **L7** (0.1 mmol) was stirred at 40 °C in 20 mL of dichloromethane for 8–10 h. The mixture was filtered and evaporated to afford red solids which were further purified by silica gel column chromatography (CH_2Cl_2–EA = 98 : 2) to afford isomers of cyclometalated compounds in yields of 82–92%.

2a: Red, 10 h, yield: 82%. Anal. Calc. for $C_{40}H_{44}Cl_2Ir_2N_2$: C 47.66, H 4.40, N 2.78. Found: C 47.37, H 4.25, N 2.71%. ^{1}H NMR (400 MHz, $CDCl_3$, ppm): δ 8.52 (d, 2H, HC═N); 8.28 (m, 2H); 7.92 (m, 2H); 7.53–7.73 (m, 4H); 7.29 (m, 2H); 7.10 (m, 2H); 1.44 (d, 30H, C_5Me_5). IR (KBr): $\nu_{C=N}$ = 1586 cm^{-1}.

2b: Red, 8 h, yield: 92%. Anal. Calc. for $C_{42}H_{48}Cl_2Ir_2N_2O_2$: C 47.23, H 4.53, N 2.62. Found: C 47.36, H 4.26, N 2.52%. ^{1}H NMR (400 MHz, $CDCl_3$, ppm): δ 8.22, 8.25 (d, 2H, HC═N); 7.06–7.63 (m, 6H); 7.39 (d, 2H); 6.61–6.64 (m, 2H); 3.93 (d, 6H, OMe); 1.51 (d, 30H, C_5Me_5). ^{13}C-NMR ($CDCl_3$, ppm): δ 174.00, 173.68 (Ir–C); 162.77, 162.73 (HC═N); 150.56, 150.53; 140.54, 140.47; 131.54, 131.47; 123.25, 123.22; 108.96, 108.94; 89.15, 89.04

Table 1 Crystal data and structure refinement for complexes (solv = unknown solvent)

	1a	**1b**·2CH_2Cl_2	**1b′**·2CH_2Cl_2	**2a**·solv	**2b**·CH_2Cl_2	**3a**·solv	**3b**·2CH_3OH	**3c**·2CH_2Cl_2·	**3c′**·2CH_2Cl_2·solv	**4a**·H_2O·solv
Empirical formula	$C_{40}H_{44}Cl_2Ir_2N_2$	$C_{44}H_{52}Cl_6Ir_2N_2O_2$	$C_{44}H_{52}Cl_6N_2O_2Rh_2$	$C_{40}H_{44}Cl_2Ir_2N_2$	$C_{43}H_{50}Cl_4Ir_2N_2O_2$	$C_{92}H_{96}F_{12}Ir_4N_8O_{12}S_4$	$C_{98}H_{112}F_{12}Ir_4N_8O_{18}S_4$	$C_{98}H_{106}Cl_4F_{12}Ir_4N_8O_{12}S_4$	$C_{98}H_{108}Cl_4F_{12}N_8O_{12}Rh_4S_4$	$C_{92}H_{98}F_{12}Ir_4N_8O_{15}S_4$
M_r	1008.07	1237.98	1059.40	1008.07	1153.05	2630.81	2815.00	2854.75	2499.60	2648.82
Crystal system	Monoclinic	Monoclinic	Monoclinic	Monoclinic	Monoclinic	Monoclinic	Monoclinic	Monoclinic	Monoclinic	Monoclinic
Space group	$P2_1/n$	$P2_1/c$	$P2_1/c$	$C2/c$	$C2/c$	$C2/c$	$P2_1/n$	$C2/c$	$P2_1/n$	$C2/m$
a/Å	7.468(3)	16.338(7)	16.297(7)	22.261(12)	27.594(9)	33.826(15)	17.03(3)	16.551(10)	11.693(10)	27.719(12)
b/Å	18.049(7)	10.244(5)	10.250(4)	8.705(5)	12.355(4)	18.632(8)	18.63(3)	34.96(2)	33.35(3)	22.208(12)
c/Å	13.623(6)	3.969(6)	14.028(6)	22.589(12)	12.452(4)	19.427(9)	17.40(3)	21.073(13)	15.824(14)	20.173(10)
β/°	101.915(5)	105.319(6)	105.111(5)	90.839(7)	96.464(4)	109.080(7)	114.60(2)	106.644(9)	109.940(12)	119.209(9)
V/Å^3	1796.8(13)	2255.0(18)	2262.3(17)	4377(4)	4218(2)	11571(9)	5020(14)	11684(12)	5800(9)	10840(9)
T/K	293	293	293	293	293	293	293	293	293	293
Z	2	2	2	4	4	4	2	4	2	4
Reflections/unique	8531/3824	10451/4818	9145/3970	10280/4686	9875/4462	23505/10174	20681/8812	22373/10252	28309/12561	25942/11808
R_{int}	0.0390	0.0500	0.0454	0.0531	0.0337	0.0982	0.1283	0.0775	0.0791	0.0699
wR_2^a	0.0471	0.0723	0.0949	0.0705	0.0765	0.1379	0.1194	0.0908	0.1540	0.1359

^{a} w$R_2 = [\sum w(|F_o^2| - |F_c^2|)^2 / \sum w|F_o^2|^2]^{1/2}$.

(C_5Me_5); 55.17 (OMe); 9.01, 8.94 (C_5Me_5). IR (KBr): $\nu_{C=N}$ = 1588 cm^{-1}.

Preparation of tetranuclear complexes 3a–3e and 3a′–3c′

Route A. Pyrazine (0.1 mmol) was added to a suspension of $[Cp^*MCl_2]_2$ (0.1 mmol, M = Ir, Rh) in CH_3OH at room temperature and stirred for 5 h. $Ag(CF_3SO_3)$ (0.4 mmol) was added to the resulting yellow precipitate and stirred for 2 h. NaOAc (0.6 mmol) and corresponding substrate **L1–L5** (0.1 mmol) were added and kept stirring for an additional 12 h. Solvent was removed in vacuum, and the residue was extracted with CH_2Cl_2. Further purification by silica gel column chromatography (CH_2Cl_2–CH_3OH = 9 : 1) afforded isomers of tetranuclear complexes as a red solids in yields of 54–58%.

Route B. $Ag(CF_3SO_3)$ (51 mg, 0.2 mmol) was added to a solution of the corresponding binuclear complex **1a–1e** or **1a′–1c′** (0.1 mmol) in CH_3OH (20 mL) at room temperature and stirred for 3 h, followed by filtration to remove insoluble materials. Pyrazine (0.1 mmol) was added to the filtrate and stirred for 12 h. The solvent was removed, and the residue was extracted with CH_2Cl_2. Further purification by silica gel column chromatography (CH_2Cl_2–CH_3OH = 9 : 1) afforded isomers of tetranuclear complexes as a red solid in yields of 60–72%.

3a: yields: 56% (route A), 72% (route B). Anal. Calc. for $C_{92}H_{96}F_{12}Ir_4N_8O_{12}S_4$: C 42.00, H 3.68, N 4.26. Found: C 41.82, H 3.63, N 4.09%. ^1H NMR (400 MHz, CD_3OD, ppm): δ 8.86 (d, 4H, HC═N); 8.29 (s, 8H, pyrazine); 8.24 (d, 4H, Ar–H); 7.49–7.58 (m, 12H, Ph); 7.28–7.30 (m, 8H, Ph); 1.52 (s, 60H, C_5Me_5). ^1H NMR (400 MHz, $CDCl_3$, ppm): δ 8.79 (s, 4H, HC═N); 8.69 (s, 4H, HC═N); 8.56 (s, 8H, pyrazine); 8.26 (s, 8H, pyrazine); 7, 50–7.01 (m, 40H, Ph); 1.56–1.51 (d, 120H, C_5Me_5). IR (KBr): $\nu_{C=N}$ = 1555 cm^{-1}.

3b: yields: 58% (route A), 75% (routed B). Anal. Calc. for $C_{96}H_{104}F_{12}Ir_4N_8O_{16}S_4$: C 41.91, H 3.81, N 4.07. Found: C 41.78, H 3.54, N 4.33%. ^1H NMR (400 MHz, $CDCl_3$, ppm): δ 8.62 (s, 4H, HC═N); 8.40 (s, 8H, pyrazine); 8.14 (d, 4H, Ar–H); 7.36 (d, 8H, Ar–H); 7.14 (d, 8H, Ar–H); 3.91 (s, 12H, OCH_3); 1.57 (s, 60H, C_5Me_5). ^1H NMR (400 MHz, $CDCl_3$, ppm): δ 8.60 (s, 4H, HC═N); 8. 51 (s, 4H, HC═N); 8.47–8.44 (d, 16H, pyrazine); 8.20–7.11 (m, 40H, Ar–H); 3.90–3.82 (d, 24H, OCH_3); 1.57–1.56 (d, 120H, C_5Me_5). IR (KBr): $\nu_{C=N}$ = 1556 cm^{-1}.

3c: yields: 54% (route A), 63% (routed B). Anal. Calc. for $C_{96}H_{104}F_{12}Ir_4N_8O_{12}S_4$: C 42.91, H 3.90, N 4.17. Found: C 42.73, H 3.71, N 4.26%. ^1H NMR (400 MHz, $CDCl_3$, ppm): δ 8.69 (s, 4H, HC═N); 8.43 (s, 8H, pyrazine); 8.28 (d, 4H, Ar–H); 7.39 (d, 8H, Ar–H); 7.06 (d, 8H, Ar–H); 2.42 (s, 12H, CH_3); 1.54 (s, 60H, C_5Me_5). ^1H NMR (400 MHz, $CDCl_3$, ppm): δ 8.63 (s, 4H, HC═N); 8.49 (s, 4H, HC═N); 8.44–8.40 (d, 16H, pyrazine); 8.19–7.10 (m, 40H, Ar–H); 2.41–2.39 (d, 24H, OCH_3); 1.56 (d, 120H, C_5Me_5). IR (KBr): $\nu_{C=N}$ = 1555 cm^{-1}.

3d: yields: 54% (route A), 60% (routed B). Anal. Calc. for $C_{92}H_{92}Cl_4F_{12}Ir_4N_8O_{12}S_4$: C 39.91, H 3.35, N 4.05. Found: C 39.65, H 3.04, N 4.02%. ^1H NMR (400 MHz, CD_3OD, ppm): δ 8.75 (s, 4H, HC═N); 8.13–8.15 (m, 12H, pyrazine and Ar–H); 7.49 (d, 8H, Ar–H); 7.22 (d, 8H, Ar–H); 1.57 (s, 60H, C_5Me_5). ^1H NMR (400 MHz, $CDCl_3$, ppm): δ 8.55 (s, 4H, HC═N); 8. 42 (s, 4H, HC═N); 8.13–7.13 (m, 56H, pyrazine and Ar–H); 1.59–1.56 (d, 120H, C_5Me_5). IR (KBr): $\nu_{C=N}$ = 1551 cm^{-1}.

3e: yields: 56% (route A), 70% (routed B). Anal. Calc. for $C_{72}H_{88}F_{12}Ir_4N_8O_{12}S_4$: C 36.29, H 3.72, N 4.70. Found C 36.11, H, 3.70, N 4.58%. ^1H NMR (400 MHz, CD_3OD, ppm): δ 8.67 (s, 4H, HC═N); 8.11 (s, 8H, pyrazine); 7.84 (s, 4H, Ph); 4.02 (s, 12H, Me); 1.69 (s, 60H, C_5Me_5). ^1H NMR (400 MHz, $CDCl_3$, ppm): δ 8.59 (s, 4H, HC═N in isomer A); 8.48 (s, 4H, HC═N in isomer B); 8.43 (s, 8H, pyrazine in isomer B); 8.12 (s, 8H, pyrazine in isomer A); 4.06 (s, 12H, Me in isomer B); 3.87 (s, 12H, Me in isomer A); 1.73 (60H, C_5Me_5 in isomer A); 1.65 (60H, (60H, C_5Me_5 in isomer B). IR (KBr): $\nu_{C=N}$ = 1536 cm^{-1}.

3a′: yields: 54% (route A), 62% (route B). Anal. Calc. for $C_{92}H_{96}F_{12}Rh_4N_8O_{12}S_4$: C 48.60, H 4.26, N 4.93. Found: C 48.81, H 4.59, N 4.79%. ^1H NMR (400 MHz, CD_3OD, ppm): δ 8.88 (d, 4H, HC═N); 8.25 (s, 8H, pyrazine); 8.20 (d, 4H, Ar–H); 7.48–7.53 (m, 12H, Ph); 7.21–7.33 (m, 8H, Ph); 1.60 (s, 60H, C_5Me_5). ^1H NMR (400 MHz, $CDCl_3$, ppm): δ 8.78 (s, 4H, HC═N); 8.67 (s, 4H, HC═N); 8.54 (s, 8H, pyrazine); 8.25 (s, 8H, pyrazine); 7.30–7.12 (m, 40H, Ph); 1.51–1.48 (d, 120H, C_5Me_5). IR (KBr): $\nu_{C=N}$ = 1556 cm^{-1}.

3b′: yields: 53% (route A), 63% (route B). Anal. Calc. for $C_{96}H_{104}F_{12}Rh_4N_8O_{16}S_4$: C 48.17, H 4.38, N 4.68. Found: C 48.10, H 4.30, N 4.53%. ^1H NMR (400 MHz, $CDCl_3$, ppm): δ 8.63 (s, 4H, HC═N); 8.41 (s, 8H, pyrazine); 8.11 (d, 4H, Ar–H); 7.36 (d, 8H, Ar–H); 7.11 (d, 8H, Ar–H); 3.93 (s, 12H, OCH_3); 1.50 (s, 60H, C_5Me_5). ^1H NMR (400 MHz, $CDCl_3$, ppm): δ 8.58 (s, 4H, HC═N); 8. 48 (s, 4H, HC═N); 8.40 (d, 16H, pyrazine); 8.18–7.16 (m, 40H, Ar–H); 3.90–3.81 (d, 24H, OCH_3); 1.57–1.56 (d, 120H, C_5Me_5). IR (KBr): $\nu_{C=N}$ = 1556 cm^{-1}.

3c′: yields: 58% (route A), 60% (routed B). Anal. Calc. for $C_{96}H_{104}F_{12}Rh_4N_8O_{12}S_4$: C 49.49, H 4.50, N 4.81. Found: C 49.40, H 4.72, N 4.76%. ^1H NMR (400 MHz, $CDCl_3$, ppm): δ 8.69 (s, 4H, HC═N); 8.40 (s, 8H, pyrazine); 8.25 (d, 4H, Ar–H); 7.28 (d, 8H, Ar–H); 7.00 (d, 8H, Ar–H); 2.41 (s, 12H, CH_3); 1.54 (s, 60H, C_5Me_5). ^1H NMR (400 MHz, $CDCl_3$, ppm): δ 8.60 (s, 4H, HC═N); 8.41 (s, 4H, HC═N); 8.40–8.35 (d, 16H, pyrazine); 8.18–7.11 (m, 40H, Ar–H); 2.40–2.39 (d, 24H, OCH_3); 1.56 (d, 120H, C_5Me_5). IR (KBr): $\nu_{C=N}$ = 1531 cm^{-1}.

Preparation of tetranuclear complexes 4a and 4b

$Ag(CF_3SO_3)$ (0.2 mmol) was added to a solution of corresponding binuclear complex **2a** and **2b** (0.1 mmol) in CH_3OH (20 mL) at room temperature and stirred for 3 h, followed by filtration to remove insoluble materials. Pyrazine (0.1 mmol) was added to the filtrate and stirred for 12 h. The solvent was removed and the residue was extracted with CH_2Cl_2. Further purification by silica gel column chromatography (CH_2Cl_2–CH_3OH = 9 : 1) afforded pure tetranuclear complexes as red solids in yields of 75–78%.

4a: Red, yield: 75%. Anal. Calc. for $C_{92}H_{96}F_{12}Ir_4N_8O_{12}S_4$: C 42.00, H 3.68, N 4.26. Found: C 41.79, H 3.31, N 4.17%. ^1H NMR (400 MHz, CD_3OD, ppm): δ 8.56 (s, 4H, HC═N); 8.44 (s, 8H, pyrazine); 7.89 (m, 4H, Ar–H); 7.89 (m, 8H, Ar–H); 7.56 (d, 4H, Ar–H); 7.37 (m, 4H, Ar–H); 7.00–7.05 (m, 4H, Ar–H); 1.29 (s, 60H, C_5Me_5). ^1H NMR (400 MHz, $CDCl_3$, ppm): δ 8.60 (s, 4H, HC═N); 8.24 (s, 8H, pyrazine); 7.83–7.81 (d, 4H, Ph); 7.58–7.56 (d, 4H, Ph); 7.40–7.38 (d, 8H, Ph); 7.17–6.98 (m, 8H, Ph); 6.70–6.67 (d, 8H, Ph); 1.26 (s, 60H, C_5Me_5). IR (KBr): $\nu_{C=N}$ = 1584 cm^{-1}.

4b: Red, yield: 78%. Anal. Calc. for $C_{96}H_{104}F_{12}Ir_4N_8O_{16}S_4$: C 41.91, H 3.81, N 4.07. Found: C 41.63, H 3.66, N 3.98%. ^{1}H NMR (400 MHz, CD_3CN, ppm): δ 8.83 (s, 4H, HC═N); 8.63 (s, 8H, pyrazine); 8.55 (m, 4H, Ar–H); 7.82 (d, 4H, Ar–H); 7.60 (d, 4H, Ar–H); 7.73 (m, 4H, Ar–H); 6.86 (m, 4H, Ar–H); 3.98 (s, 12H, OCH_3); 1.60 (s, 60H, C_5Me_5). ^{1}H NMR (400 MHz, $CDCl_3$, ppm): δ 8.75 (s, 4H, HC═N); 8.42 (s, 8H, pyrazine); 8.16–7.59 (m, 8H, Ph); 7.36–7.35 (d, 8H, Ph); 7.11–6.68 (m, 12H, Ph); 1.43 (s, 60H, C_5Me_5).IR (KBr): $\nu_{C=N}$ = 1586 cm^{-1}.

X-Ray crystallography

All single crystals were obtained from slow diffusion of hexane or diethyl ether into CH_2Cl_2 or CH_3OH solutions of the corresponding compounds. All the determinations of unit cell and intensity data were performed with graphite-monochromated Mo-Kα radiation (λ = 0.71073 Å). All the data were collected at room temperature using the ω scan technique. These structures were solved by direct methods, using Fourier techniques, and refined on F^2 by a full-matrix least-squares method. All the calculations were carried out with the SHELXTL[18] program.

The pentamethylcyclopentadienyl ligand of complex **2a** was strongly disordered because of rotation at room temperature, and it was also refined to two idealized positions (68 : 32). The 120 thermal parameters of 20 atoms, (C11–C20/C11′–C20′), were restrained. Some unknown solvents are strongly disordered and cannot be refined properly, as a result, the SQUEEZE[19] algorithm was used to omit all of these disordered fragments.

In complex **2b**, two restraints were used to restrain both bond distance of C22–Cl2 and angle distance of Cl2 Cl2_#1 (symmetry code #1: 2 – x, y, 3/2 – z).

In complex **3a**, all atoms of the two triflate anions were refined isotropically because of non-positive definition and other non-hydrogen atoms were refined anisotropically. Two of the four triflate anions and some unknown solvents are strongly disordered and cannot be refined properly, as a result, the SQUEEZE[19] algorithm was used to omit all of these disordered fragments. Three pairs of atoms (O2, S1, F2, and O2′ S1′, F2′) with C45/S1 triflate anion and all O and F atoms with C46/S2 were treated using a disorder mode. All 67 restraints were used to restrain the geometry of both triflate anions (C45/S1, C45′/S1′ and C46/S2) to get better results.

Because the diffraction points are not very high quality and there is some trailing, the error of refinement of complex **3b** is slightly larger, as a result, the reported parameters on the unit cell axes are also large.

In complex **3c**, the bond distance of C47–F2 was restrained so that the geometry of the triflate anion was improved, the thermal ellipsoids of atom N1 was restrained, 13 least-squares restraints were used, of which 12 thermal parameters of C47 and N1, and one bond distance C47–F2 were restrained. Some unknown solvents are strongly disordered and cannot be refined properly, as a result, the SQUEEZE[19] algorithm was used to omit all of these disordered fragments.

In the asymmetric unit of complex **4a**, two of the four triflate anions and some unknown solvents are strongly disordered and cannot be refined properly, as a result, the SQUEEZE[19] algorithm was used to omit all of these disordered fragments. The H atoms of the water molecule could not restrained and were deleted. Eight least-squares restraints were used, which corresponding to six thermal parameters of C46 and two bond distances of S2–C46. The cell contents ($C_{368}H_{392}N_{32}O_{52}F_{48}S_{16}Ir_{16}$) include the atoms in the absence of two triflate anions.

In all complexes, hydrogen atoms which could be found were placed in geometrically calculated positions with fixed isotropic thermal parameters.

Acknowledgements

This work was supported by the National Science Foundation of China (20721063), Shanghai Science and Technology Committee (08DZ2270500, 08DJ1400103), Shanghai Leading Academic Discipline Project (B108), and the National Basic Research Program of China (2009CB825300, 2010DFA41160).

References

1 For reviews, see: (*a*) D. L. Caulder and K. N. Raymond, *Acc. Chem. Res.*, 1999, **32**, 975; (*b*) G. F. Swiegers and T. J. Malefetse, *Chem. Rev.*, 2000, **100**, 3483; (*c*) F. A. Cotton, C. Lin and C. A. Murillo, *Acc. Chem. Res.*, 2001, **34**, 759; (*d*) B. J. Holliday and C. A. Mirkin, *Angew. Chem., Int. Ed.*, 2001, **40**, 2022; (*e*) C. H. M. Amijs, G. P. M. van Klink and G. van Koten, *Dalton Trans.*, 2006, 308; (*f*) J. L. Boyer, M. L. Kuhlman and T. B. Rauchfuss, *Acc. Chem. Res.*, 2007, **40**, 233; (*g*) B. H. Northrop, H.-B. Yang and P. J. Stang, *Chem. Commun.*, 2008, 5896; (*h*) E. Zangrando, M. Casanova and E. Alessio, *Chem. Rev.*, 2008, **108**, 4979; (*i*) S. J. Lee and W. Lin, *Acc. Chem. Res.*, 2008, **41**, 521; (*j*) M. Yoshizawa, J. K. Klosterman and M. Fujita, *Angew. Chem., Int. Ed.*, 2009, **48**, 3418.
2 Selected examples include: (*a*) M. M. Olmstead, M. F. Maestre and R. H. Fish, *J. Am. Chem. Soc.*, 1992, **114**, 10647; (*b*) K. K. Klausmeyer, S. R. Wilson and T. B. Rauchfuss, *J. Am. Chem. Soc.*, 1999, **121**, 2705; (*c*) K. Yamanari, S. Yamamoto, R. Ito, Y. Kushi, A. Fuyuhiro, N. Kubota, T. Fukuo and R. Arakawa, *Angew. Chem., Int. Ed.*, 2001, **40**, 2268; (*d*) P. H. Dinolfo and J. T. Hupp, *Chem. Mater.*, 2001, **13**, 3113; (*e*) Y. Yamamoto, H. Suzuki, N. Tajima and K. Tatsumi, *Chem.–Eur. J.*, 2002, **8**, 4734; (*f*) V. Blanco, M. Chas, D. Abella, C. Peinador and J. M. Quintela, *J. Am. Chem. Soc.*, 2007, **129**, 13978; (*g*) R.-T. Liao, W.-C. Yang, P. Thanasekaran, C.-C. Tsai, M. Sathiyendiran, Y.-H. Liu, T. Rajendran, H.-M. Lin, T.-W. Tseng and K.-L. Lu, *Chem. Commun.*, 2008, 3175; (*h*) A. Rit, T. Pape and F. E. Hahn, *J. Am. Chem. Soc.*, 2010, **132**, 4572.
3 K. Severin, *Chem. Commun.*, 2006, 3859.
4 B. Therrien, *Eur. J. Inorg. Chem.*, 2009, 2445.
5 Y.-F. Han, W.-G. Jia, W.-B. Yu and G.-X. Jin, *Chem. Soc. Rev.*, 2009, **38**, 3419.
6 Y.-F. Han, W.-G. Jia, Y.-J. Lin and G.-X. Jin, *Angew. Chem., Int. Ed.*, 2009, **48**, 6.
7 (*a*) M.-L. Lehaire, R. Scopelliti, H. Piotrowski and K. Severin, *Angew. Chem., Int. Ed.*, 2002, **41**, 1419; (*b*) G.-L. Wang, Y.-J. Lin, H. Berke and G.-X. Jin, *Inorg. Chem.*, 2010, **49**, 2193.
8 B. Therrien, G. Süss-Fink, P. Govindaswamy, A. K. Renfrew and P. J. Dyson, *Angew. Chem., Int. Ed.*, 2008, **47**, 3773.
9 (*a*) Y.-F. Han, Y.-J. Lin, W.-G. Jia and G.-X. Jin, *Organometallics*, 2008, **27**, 4088; (*b*) Y.-F. Han, Y.-J. Lin, W.-G. Jia, G.-L. Wang and G.-X. Jin, *Chem. Commun.*, 2008, 1807; (*c*) W.-G. Jia, Y.-F. Han, Y.-J. Lin, L.-H. Weng and G.-X. Jin, *Organometallics*, 2009, **28**, 3459; (*d*) W.-Z. Zhang, Y.-F. Han, Y.-J. Lin and G.-X. Jin, *Dalton Trans.*, 2009, 8426.
10 Y.-F. Han, H. Li, L.-H. Weng and G.-X. Jin, *Chem. Commun.*, 2010, **46**, 3556.
11 (*a*) T. Kajimoto and J. Tsuji, *J. Org. Chem.*, 1983, **48**, 1685; (*b*) J. Lewkowski and M. Dziegielewski, *Heteroat. Chem.*, 2010, **20**, 431; (*c*) B. J. E. Reich, A. K. Justice, B. T. Beckstead, J. H. Reibenspies and S. A. Miller, *J. Org. Chem.*, 2004, **69**, 1357; (*d*) S. Sellarajah, T. Lekishvili, C. Bowring, A. R. Thompsett, H. Rudyk, C. R. Birkett, D. R. Brown and I. H. Gilbert, *J. Med. Chem.*, 2004, **47**, 5515.
12 D. L. Davies, O. Al-Duaij, J. Fawcett, M. Giardiello, S. T. Hilton and D. R. Russell, *Dalton Trans.*, 2003, 4132.
13 L. Li, W. W. Brennessel and W. D. Jones, *Organometallics*, 2009, **28**, 3492.

14 L. Li, W. W. Brennessel and W. D. Jones, *J. Am. Chem. Soc.*, 2008, **130**, 12414.
15 A. D. Ryabov, *Chem. Rev.*, 1990, **90**, 403.
16 W.-B. Yu, Y.-F. Han, Y.-J. Lin and G.-X. Jin, *Organometallics*, 2010, **29**, 2827.
17 C. White, A. Yates and P. M. Maitles, *Inorg. Synth.*, 1992, **29**, 228.
18 G. M. Sheldrick, *SHELXL-97*, Universität Göttingen, Germany, 1997.
19 (*a*) P. Van Der Sluis and A. L. Spek, *Acta Crystallogr., Sect. A: Found. Crystallogr.*, 1990, **46**, 194; (*b*) A. L. Spek, *PLATON, A Multipurpose Crystallographic Tool*, Utrecht University, Utrecht, The Netherlands, 2005; (*c*) Farrugia, *WINGX*, 1999.